Communication (heading)

Isoelectric Point-Controlled Preferential Photodeposition of Platinum on Cu_2O-TiO_2 Composite Surfaces

Mei Wang [a], Yuanxu Liu [b], Dan Li [a], Junwang Tang [c], Weixin Huang*[a]

[a] *Hefei National Laboratory for Physical Sciences at the Microscale, CAS Key Laboratory of Materials for Energy Conversion and Department of Chemical Physics, University of Science and Technology of China, Hefei 230026, P. R. China.*
[b] *School of Pharmacy, Anhui University of Chinese Medicine, Anhui Academy of Chinese Medicine, Hefei 230012, P.R. China.*
[c] *Department of Chemical Engineering, University College London, Torrington Place, London WC1E 7JE, U.K.*

ARTICLE INFO

Article history:
Received
Received in revised form
Accepted
Available online

Keywords:
Photocatalysts
Photocatalytic water reduction
Selective adsorption
Oxide composite
Co-catalyst

ABSTRACT

Photodeposition emerges as a convenient method to synthesize metal particles on semiconductor supports. In this work, we study the photodeposition of Pt on Cu_2O-TiO_2 composite surfaces employing H_2PtCl_6 aqueous solution as the precursor and reveal a key role of isoelectric point of oxide surfaces on the Pt photodeposition process. Under the photodeposition conditions, Pt metal particles are facilely photodeposited on TiO_2 support; on Cu_2O-TiO_2 composite supports, the Cu_2O surface is positively charged and enriched with photo-excited holes while the TiO_2 surface is negatively charged and enriched with photo-excited electrons. This lead to the preferential adsorption of $PtCl_6^{2-}$ anion precursor on the Cu_2O surface of Cu_2O-TiO_2 composite and the dominant formation of Pt oxide particles on Cu_2O surface but few Pt metal particles on TiO_2 surface. Consequently, the activity of resulting Pt/Cu_2O-TiO_2 composite photocatalysts in photocatalytic water reduction decreases as the Cu_2O content increases. These results deepen the understanding of photodeposition processes on oxide composite surfaces.

Photocatalytic water splitting has been extensively studied as an ideal method to produce hydrogen since the report of the Honda-Fujishima effect of water splitting using a TiO_2 electrode [1]. It consists of photoexcitation of semiconductor photocatalyst to generate electrons and holes in the bulk, transfer of photoexcited carriers from the bulk to the surface, and photoexcited electrons-participated water reduction to H_2 and photoexcited holes-participated water oxidation to O_2 on the surface [2-4]. Among various semiconductor photocatalysts for photocatalytic water splitting, TiO_2 is considered as a potential commercial photocatalyst due to the favorable electronic energy band structure and high photo-chemical stability [5-7]. However, TiO_2 photocatalyst suffers from the wide band gap of around 3.2 eV [8-10] and rapid recombination of photoexcited electron-hole pairs [5,6]. Great effort has been thus devoted to suppressing the recombination of photoexcited electron-hole pairs to increase the efficiency of TiO_2 in photocatalytic water splitting, and the co-catalyst strategy is very effective. Noble metals (Pt, Pd, Au and Ag) and transitional metal oxides have been demonstrated as efficient co-catalysts for TiO_2 to suppress the charge recombination via the transfer of photoexcited electrons and holes from TiO_2 to the co-catalyst, respectively [11-20]. Recently space-separated noble metal and transitional metal oxide co-catalysts have been successfully loaded on TiO_2 to allow simultaneous transfer of photoexcited electrons and holes from TiO_2 respectively to the noble metal and transitional metal oxide co-catalysts [11-13].

Utilizing photoexcited electrons to reduce metal cations, photodeposition emerges as a convenient method to load metal particles on semiconductors [21-28]. Photodeposition was also successfully used for a simultaneous loading of Au and CoO_x respectively on electron-enriched {010} face and hole-enriched {110} face of $BiVO_4$ nanocrystals [11]. However, there are few works reported on photodeposition of metal particles on oxide composite surfaces. Cu_2O acts as a nice hole-scavenger co-catalyst for TiO_2 [29-31]. In this letter, we report the structures and photocatalytic performances in water reduction of Pt/Cu_2O-TiO_2 composite photocatalysts prepared by photodeposition of Pt particles on Cu_2O-TiO_2 composite surfaces. The results reveal an interesting isoelectric point-controlled preferential adsorption and photodeposition of Pt species on Cu_2O-TiO_2 composite surfaces.

Experimental details are described in the Supporting Information. Pt with loadings of about 0.5% was photodeposited on TiO_2 and Cu_2O-TiO_2 composites employing H_2PtCl_6 aqueous solutions as the Pt precursor. Under the photodeposition

condition, the pH values of the solutions were measured to be 3.6. Table 1 summarizes compositions and BET specific surface areas of various photocatalysts. Both Pt loadings and BET specific surface areas are similar for all photocatalysts. Fig.1. shows photocatalytic H_2 productions as a function of reaction time of various photocatalysts in photocatalytic water reduction illuminated with simulated solar light. It can be seen that the photocatalytic H_2 production increases linearly with the reaction time for various photocatalysts, indicating the stability of these photocatalysts. The calculated mass-specific photocatalytic H_2 production rates of all photocatalysts are summarized in Table 1. 0.5%Pt/TiO_2 exhibits a H_2 production rate of 4.8 $mmol^{-1}g^{-1}h^{-1}$, but the H_2 production rate of Pt-Cu_2O-TiO_2 composite photocatalysts keeps decreasing with the loading of Cu_2O. These results suggest that the Pt and Cu_2O species in Pt/Cu_2O-TiO_2 composite photocatalysts exert a negative effect, instead of a synergetic effect, on promoting the photocatalytic performance of TiO_2.

Table 1 Compositions, BET specific surface areas and mass-specific photocatalytic H_2 productions of various photocatalysts.

Samples	Cu loading (wt%)	Pt loading (wt%)	BET (m^2/g)	H_2 Production ($mmol\ g^{-1}h^{-1}$)
0.5%Pt/TiO_2		0.59	76.2	4.8
Pt/0.005%Cu_2O-TiO_2	0.01	0.49	69.8	3.9
Pt/0.05%Cu_2O-TiO_2	0.07	0.42	70.1	3.2
Pt/0.5%Cu_2O-TiO_2	0.70	0.50	77.7	1.6
Pt/1%Cu_2O-TiO_2	1.26	0.50	72.5	0.7

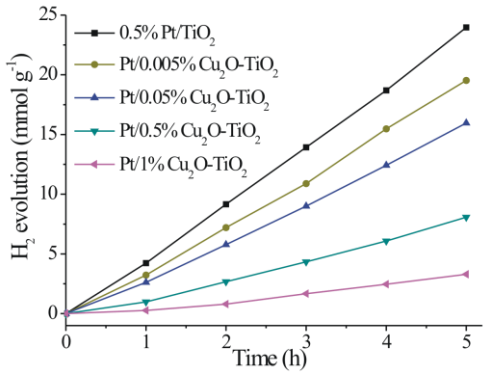

Fig. 1. Photocatalytic H_2 production as a function of reaction time of various Pt/Cu_2O-TiO_2 under simulated solar light irradiation.

Fig. 2A shows XRD patterns of various photocatalysts, in which all observed diffraction patterns could be indexed to anatase TiO_2 (JCPDS card: 21-1272). No peaks associated with Cu or Pt species could be identified. This may be due to the fine dispersions of copper and platinum species on TiO_2 and/or the low loadings of copper and platinum in all photocatalysts. Surface structures of all photocatalysts were characterized with XPS. As shown in Fig. S1, all Pt/Cu_2O-TiO_2 composite photocatalysts exhibit the same Ti $2p_{3/2}$ binding energy at 458.8 eV and Cu $2p_{3/2}$ binding energy at 932.4 eV that respectively correspond to TiO_2 and Cu_2O [30]. However, they exhibit Cu_2O loading-dependent Pt 4f XPS features (Fig. 2B). A peak at around 75.6 eV corresponds to an energy loss peak of TiO_2, and other peaks at 70.9/74.3, 72.8/76.1, and 74.2/77.5 eV can be assigned to the $4f_{7/2}/4f_{5/2}$ components of metallic Pt, Pt^{2+}, and Pt^{4+} species, respectively [32-34]. Fig. 2C shows the Pt speciation in various photocatalysts. 0.5%Pt/TiO_2 exhibits dominant metallic Pt species with minor Pt^{2+} species. With the Cu_2O loading of Pt/Cu_2O-TiO_2 increasing, the metallic Pt species decreases and could not be observed in Pt/1%Cu_2O-TiO_2; the Pt^{2+} species increases, reaches the maximum in Pt/0.5%Cu_2O-TiO_2 and then slightly decreases in Pt/1%Cu_2O-TiO_2; and the Pt^{4+} species emerges in Pt/1%Cu_2O-TiO_2. These XPS results demonstrate that the Pt species changes from the metallic Pt to the Pt cations in our Pt/Cu_2O-TiO_2 photocatalysts prepared by photodeposition as the Cu_2O loading increases.

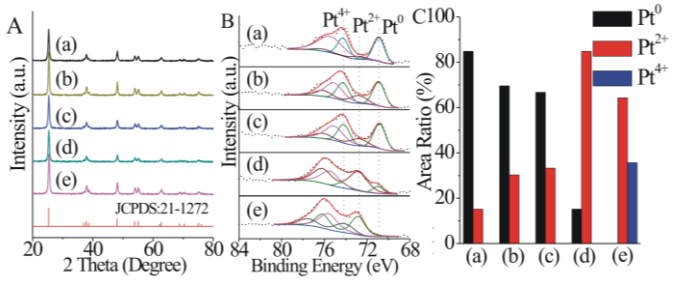

Fig. 2. (A) XRD patterns, (B) Pt 4f XPS spectra with peak-fitting results, and (C) calculated Pt speciation of (a) 0.5%Pt/TiO_2, (b) Pt/0.005%Cu_2O-TiO_2, (c) Pt/0.05%Cu_2O-TiO_2, (d) Pt/0.5%Cu_2O-TiO_2 and (e) Pt/1%Cu_2O-TiO_2 photocatalysts. The red line in Fig. 2A represents the standard XRD pattern of anatase TiO_2 (JCPDS Card No. 21-1272). The scatter points and solid lines in Fig. 2B respectively represent the original XPS spectra and peak-fitted XPS spectra.

Representative TEM and HRTEM images of Pt/TiO_2 and Pt/Cu_2O-TiO_2 photocatalysts are shown in Fig. 3, Fig. S2 and Fig. S3. The identified lattice spacings of 0.35, 0.21, 0.23, 0.26 and 0.22 nm arise from TiO_2(101), Cu_2O(200), Pt(111), PtO(101) and PtO_2(011), respectively [29,30,35,36]. Fig. S3 gives FT-transformed patterns of TRTEM images of individual particles to distinguish nanoparticles with similar observed lattice spacings. As reported in our previous paper [29], TiO_2 exhibits a rod shape, and Cu_2O forms a thin film on TiO_2 in Cu_2O-TiO_2 composites up to 1%Cu_2O-TiO_2, forming TiO_2 (core)/Cu_2O (thin film shell) rod structures in which the Cu_2O shell thickness increases with the Cu_2O loading. Pt/TiO_2 and Pt/Cu_2O-TiO_2 photocatalysts remain rod shapes, and Cu_2O exists as thin layers on TiO_2 in all Pt/Cu_2O-TiO_2 photocatalysts, but exposed TiO_2 surfaces are always present. This is also confirmed by the DRIFTS results of CO adsorption on Pt/Cu_2O-TiO_2 photocatalysts (Fig. S4) in which the vibrational band of CO adsorption at Ti(IV) sites is observed for Pt/Cu_2O-TiO_2 photocatalysts [37]. Thus the original TiO_2 (core)/Cu_2O (thin film shell) rod structures of Cu_2O-TiO_2 composites get destroyed after the photodeposition processes in H_2PtCl_6 aqueous solutions. Metallic Pt nanoparticles of 2-3 nm can be easily identified in Pt/TiO_2, Pt/0.005%Cu_2O-TiO_2 and Pt/0.05%Cu_2O-TiO_2 but few PtO nanoparticles is found although the XPS results suggest the presence of minor PtO species. This could be attributed to the generally much higher dispersion of Pt oxides than Pt metal supported on oxide surfaces. In Pt/0.5%Cu_2O-TiO_2 and Pt/1%Cu_2O-TiO_2 photocatalysts with Pt oxides as the dominant Pt species, PtO and PtO_2 nanoparticles of 3-4 nm are easily observed but Pt nanoparticles can only be occasionally found. It is found that the Pt species supported on TiO_2 are always metallic Pt nanoparticles while those supported on Cu_2O include metallic Pt nanoparticles in Pt/0.005%Cu_2O-TiO_2 and Pt/0.05%Cu_2O-TiO_2 but then are exclusively PtO and PtO_2 nanoparticles in Pt/0.5%Cu_2O-TiO_2 and Pt/1%Cu_2O-TiO_2. Meanwhile, much more Pt species are photodeposited on the Cu_2O surface of Cu_2O-TiO_2 composites than on the TiO_2 surface. This agrees with the XPS results of dominant Pt oxides species since the photodeposited Pt species on TiO_2 is mainly metallic Pt nanoparticles.

The above spectroscopic and microscopic characterization results demonstrate that the presence of Cu_2O layers on TiO_2 strongly affects the photodeposition processes of Pt. The photodeposited Pt species is preferentially formed on the Cu_2O

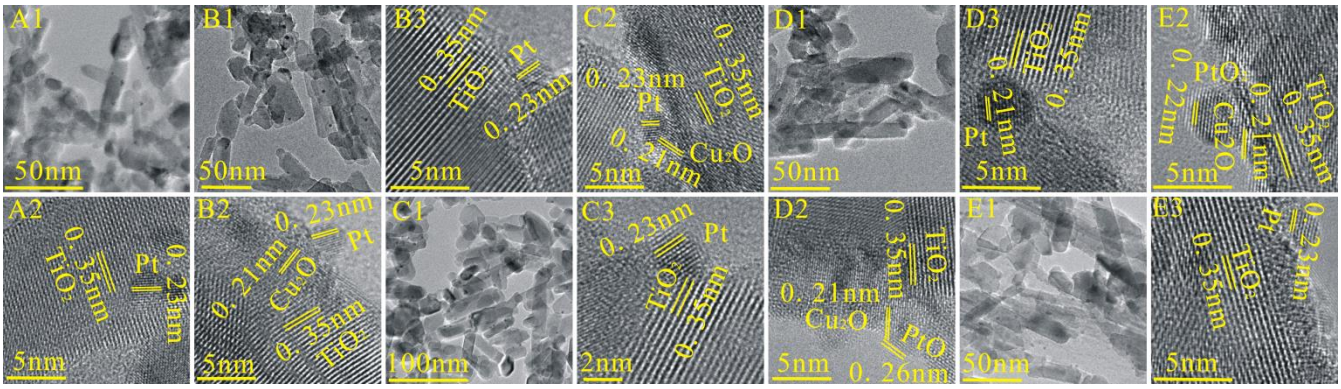

Fig.3. Representative TEM and HRTEM images of (A1 and A2) 0.5%Pt/TiO_2,(B1, B2, B3) Pt/0.005%Cu_2O-TiO_2,(C1, C2, C3) Pt/0.05%Cu_2O-TiO_2, (D1, D2, D3) Pt/0.5%Cu_2O-TiO_2, and (E1, E2, E3) Pt/1%Cu_2O-TiO_2. Lattice spacings of 0.35, 0.21, 0.23, 0.26 and 0.22 nm correspond to TiO_2(101), Cu_2O(200), Pt(111), PtO(101) and PtO_2(011), respectively.

surface, and changes from metallic Pt nanoparticles to PtO and PtO_2 nanoparticles as the Cu_2O layers thicken. It is reasonable that the synthesized Pt/Cu_2O-TiO_2 photocatalysts with dominant PtO and PtO_2 nanoparticles on Cu_2O surface and few Pt nanoparticles on TiO_2 surface are less active than the synthesized Pt/TiO_2 catalyst with Pt nanoparticles in photocatalytic water reduction, as experimentally observed.

During the photodeposition process, the $[PtCl_4]^{2-}$ precursor needs to adsorb on the oxide surface prior its photoreduction. Depending on its isoelectric point and the pH value of aqueous solution, an oxide surface in the aqueous solution is negatively, neutrally, or positively charged. We measured Zeta potentials of TiO_2, Cu_2O, and various Cu_2O/TiO_2 composites as a function of pH values (Fig. 4), from which the isoelectric point of TiO_2, 0.005%Cu_2O/TiO_2, 0.05%Cu_2O/TiO_2, 0.5%Cu_2O/TiO_2, 1%Cu_2O/TiO_2 and commercial Cu_2O is determined as 3.1, 4.8, 5.3, 5.8, 7.1 and 10.2, respectively. The pH value of employed $H_2[PtCl_4]$ aqueous solution is measured to be 3.6, thus the TiO_2 surface of Cu_2O-TiO_2 composites is locally negatively charged while the Cu_2O surface is locally strongly positively charged. Based on these observations, we proposed a photodeposition mechanism of Pt on Cu_2O-TiO_2 composites (Fig. 5). Under the employed photodeposition conditions, the negatively-charged $[PtCl_4]^{2-}$ precursor adsorb majorly on the strongly positively-charged Cu_2O surface of Cu_2O-TiO_2 composites but minorly on the negatively-charged TiO_2 surface, resulting in the preferential adsorption of $[PtCl_4]^{2-}$ precursor on Cu_2O surface of Cu_2O-TiO_2 composites. Illuminated with light, both Cu_2O and anatase TiO_2 are photoexcited to produce the electron-hole carriers, and the excited electrons in the conduction band of Cu_2O tend to transfer to the conduction band of TiO_2 at the Cu_2O-TiO_2 junction interface while the excited holes in the valence band of TiO_2 tend to transfer to the valence band of Cu_2O. This leads to electron-rich TiO_2 and hole-rich Cu_2O in Cu_2O-TiO_2 composites. Thus, the $[PtCl_4]^{2-}$ species on electron-rich TiO_2 surface can be facilely reduced to form metallic Pt nanoparticles while those on hole-rich Cu_2O surface can not be adequately reduced and tend to form PtO nanoparticles and even PtO_2 nanoparticles. The reduction extent of $[PtCl_4]^{2-}$ species on Cu_2O surface decreases as its thickness on TiO_2 increases. Thus, oxide isoelectric point plays an important role in the photodeposition of Pt on Cu_2O-TiO_2 composite surfaces via preferential adsorption of $[PtCl_4]^{2-}$ precursor. These reveal the important role of surface chemistry in photo-induced chemical processes on solid surfaces [38].

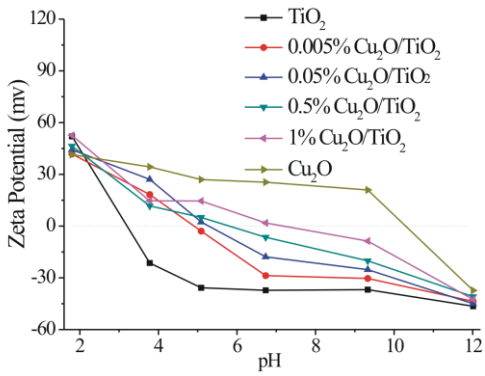

Fig. 4. Zeta potentials of TiO_2, Cu_2O, and various Cu_2O/TiO_2 composites as a function of pH values of aqueous solution.

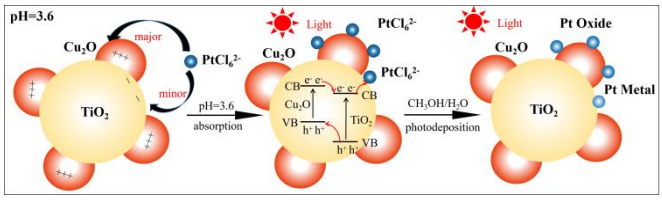

Fig.5. Schematic illustration of the photodeposition process of H_2PtCl_6 on Cu_2O/TiO_2 composite. The yellow, red, blue spheres represent TiO_2, Cu_2O, Pt species, respectively.

In summary, we have successfully investigated the photodeposition processes of Pt on Cu_2O-TiO_2 composite surfaces employing H_2PtCl_6 aqueous solution as the precursor and revealed a key role of oxide isoelectric point-controlled adsorption of $[PtCl_4]^{2-}$ precursor in the photodeposition of Pt on Cu_2O-TiO_2 composites. Under the photodeposition conditions, the $PtCl_6^{2-}$ precursor adsorb dominantly on positively-charged and hole-enriched Cu_2O surface of Cu_2O-TiO_2 composites, but minorly on negatively-charged and electron-enriched TiO_2 surface. This leads to the dominant formation of Pt oxide particles on Cu_2O surface but few Pt metal particles on TiO_2 surface. Consequently, the activity of resulting Pt/Cu_2O-TiO_2 composite photocatalysts in photocatalytic water reduction decreases as the Cu_2O content increases. These results deepen the understanding of photodeposition processes on oxide composite surfaces.

Acknowledgements.

This work was financially supported by the National Key R & D Program of Ministry of Science and Technology of China (No. 2017YFB0602205), the National Natural Science Foundation of China (Nos. 21525313, 91745202, 21703001) and the Changjiang Scholars Program of Ministry of Education of China.

Supplementary material

Experimental section, Fig. S1, Fig. S2, Fig. S3 and Fig. S4.

Reference

[1] A. Fujishima, K. Honnda, Nature 238 (1972) 37-38.
[2] T. Hisatomi, T. Minegishi, K. Domen, Bull. Chem. Soc. Jpn. 85 (2012) 647-655.
[3] T. Hisatomi, J. Kubota, K. Domen, Chem. Soc. Rev. 43(2014) 7520-7535.
[4] F. Xiong, Z.M. Wang, Z.F. Wu, et al., Sci. China Chem. doi: 10.1007/s11426-018-9377-x.
[5] J. Sun, D.K. Zhong, D.R. Gamelin, Energy Environ. Sci. 3 (2010) 1252-1261.
[6] J.F. Zhu, M. Zäch, Curr. Opin. Colloid Interface Sci. 14 (2009) 260-269.
[7] N.-L. Wu, M.-S. Lee, Int. J. Hydrogen Energy 29 (2004) 1601-1605.
[8] K. Lalitha, J.K. Reddy, M.V.P. Sharma, V.D. Kumari, M. Subrahmanyam, Int. J. Hydrogen Energy 35 (2010) 3991-4001.
[9] T.T. Le, M.S. Akhtar, D.M. Park, J.C. Lee, O.-B. Yang, Appl. Catal. B-Environ. 111 (2012) 397-401.
[10] Y. Lin, Z.Y. Jiang, C.Y. Zhu, et al., Int. J. Hydrogen Energy 38 (2013) 5209-5214.
[11] Y. Qi, Y. Zhao, Y. Y. Gao, et al., Joule 2 (2018) 1-10.
[12] R.T. Chen, S. Pang, H. Y. An, et al., Nature Energy 3 (2018) 655-663.
[13] J.K. Zhang, Z.B. Yu, Z. Gao, et al., Angew. Chem. Int. Ed. 56 (2017) 816- 820.
[14] Q. Zhang, Z. Li, S.Y. Wang, et al., ACS Catal. 6 (2016) 2182-2191.
[15] J.H. Yang, D.E. Wang, H.X. Han, C. Li, Acc. Chem. Res. 46 (2013) 1900-1909.
[16]J.R. Ran, J. Zhang, J.G. Yu, M. Jaroniec, S.Z. Qiao, Chem. Soc. Rev. 43 (2014) 7787-7812.
[17] R.G. Li, F.X. Zhang, D.E. Wang, et al., Nat. Commun. 4 (2013) 1432.
[18] S. Mubeen, J. Lee, N. Singh, et al., Nat. nanotechnol. 8 (2013) 247.
[19] D.A. Wang, T. Hisatomi, T. Takata, et al., Angew. Chem. Int. Ed. 52 (2013) 11252-11256.
[20] B.J. Ma, F.Y. Wen, H.F. Jiang, et al., Catal. Lett. 134 (2010) 78-86.
[21] A.A. Ismail, D.W. Bahnemann, S.A. Al-Sayari, Appl. Catal. A 431 (2012) 62-68.
[22] É. Karácsonyi, L. Baia, A. Dombi, et al., Catal. Today 208 (2013) 19-27.
[23] M. Maicu, M. Hidalgo, G. Colón, J.A. Navío, J. Photochem. Photobiol., A 217 (2011) 275-283.
[24] T. Sano, N. Negishi, K. Uchino, et al., J. Photochem. Photobiol., A 160 (2003) 93-98.
[25] G.M. Ma, J.Y. Liu, T. Hisatomi, et al., Chem. Commun. 51 (2015) 4302-4305.
[26] Z. Jiang, Z.Y. Zhang, W.F. Shangguan, et al., Catal. Sci. Technol. 6 (2016) 81-88.
[27] B. Kraeutler, A.J. Bard, J. Am. Chem. Soc. 100 (1978) 4317-4318.
[28] R.W. Liang, F.F. Jing, L.J. Shen, N. Qin, L. Wu, Nano Res. 8 (2015) 32 37-3249.
[29] Y.X. Liu, B.S. Zhang, L.F. Luo, et al., Angew. Chem. Int. Ed. 127 (2015) 15475-15480.
[30] Y.X. Liu, Z.L. Wang, W.X. Huang, Appl. Surf. Sci. 389 (2016) 760-767.
[31] Z.L. Wang, Y.X. Liu, D.J. Martin, et al., Phys. Chem. Chem. Phys. 15 (2013) 14956-14960.
[32] T.B. Zhou, H. Wang, S. Ji, V. Linkov, R.F. Wang, J. Power Sources 248 (2014) 427-433.
[33] D.P. He, Y.L. Jiang, H.F. Lv, M. Pan, S.C. Mu, Appl. Catal. B 132 (2013) 379-388.
[34] S. Liang, Y.M. Zhou, W.T. Wu, et al., J. Photochem. Photobiol., A 346 (2017) 168-176.
[35] L.H. Yu, Y. Shao, D.Z. Li, Appl. Catal. B 204 (2017) 216-223.
[36] X.Y. Yang, Y. Li, P. Zhang, et al., ACS Appl. Mat. Interfaces 10 (2018) 23154-23162.
[37] D. Li, S.L. Chen, R. You, et al., J. Catal. 368 (2018) 163-171.
[38] W.X. Huang, Zili Wu, Junwang Tang, W. Wei, X. F. Guo, Chin. Chem. Lett. 29 (2018) 725-726.